A peer-reviewed open-access journal
NeoBiota
Advancing research on alien species and biological invasions

NeoBiota 109: 177–201 (2026)
DOI: 10.3897/neobiota.109.192296

Research Article

Assessing invasion risk of two North American *Saperda* species (Coleoptera, Cerambycidae) in Europe using joint bioclimatic-habitat species distribution models and maritime-inland connectivity

Enrico Ruzzier[1,2,3], Davide Rassati[4], Andrea Di Giulio[1,3], Giacomo Santoiemma[4], Deepa S. Pureswaran[5], Jon Sweeney[5], Luciano Bani[2,3,6]

1 *Department of Science, Roma Tre University, Rome, Italy*
2 *World Biodiversity Association (WBA), Verona, Italy*
3 *National Biodiversity Future Center (NBFC), Palermo, Italy*
4 *Department of Agronomy, Food, Natural resources, Animals, Environment (DAFNAE), University of Padua, Padova, Italy*
5 *Natural Resources Canada, Canadian Forest Service, Atlantic Forestry Center, Fredericton, New Brunswick, Canada*
6 *Department of Earth and Environmental Sciences, University of Milano-Bicocca, Milan, Italy*

Corresponding author: Enrico Ruzzier (enrico.ruzzier@uniroma3.it)

Abstract

The introduction and establishment of non-native wood-boring insects pose a significant threat to forest ecosystems, urban trees and agricultural systems worldwide. In this study, we assessed the invasion risk of two North American longhorn beetles, *Saperda candida* and *Saperda tridentata*, to Europe by integrating joint bioclimatic–habitat species distribution models with maritime connectivity data. Both species can infest live trees; *S. candida* is primarily associated with hosts in the Rosaceae, whereas *S. tridentata* mainly attacks *Ulmus* species, making both species of primary phytosanitary concern to Europe. We developed ensemble models that separately quantified the effects of broad-scale climatic variables and fine-scale habitat factors, including land cover and host plant availability and then combined them into overall suitability maps. These were further integrated with a proxy of propagule pressure, based on international shipping connectivity to generate spatially explicit invasion risk maps. Both species showed strong model performance and high transferability. Results indicate that large areas of Europe, particularly central and western regions, offer suitable environmental conditions for establishment, although climatic constraints limit suitability in southern and northern extremes. Host plant availability emerged as a key determinant of habitat suitability, while climate acted as the primary limiting factor in Europe. When combined with maritime connectivity, invasion risk was highest in central Europe, especially in regions with dense trade networks and high environmental suitability. Our findings highlight that invasion risk is driven by the interaction between environmental suitability and human-mediated pathways, emphasising the importance of integrating ecological modelling with trade data. This approach provides a robust framework for improving surveillance, prioritising high-risk areas and supporting preventative phytosanitary strategies against invasive wood-boring insects.

Key words: Bioclimatic suitability model, Cerambycidae, habitat suitability model, host plants, insect pest, invasive species, Species Distribution Model (SDM)

Academic editor: Victoria Lantschner
Received: 26 March 2026
Accepted: 6 August 2026
Published: 17 September 2026

Citation: Ruzzier E, Rassati D, Di Giulio A, Santoiemma G, Pureswaran DS, Sweeney J, Bani L (2026) Assessing invasion risk of two North American *Saperda* species (Coleoptera, Cerambycidae) in Europe using joint bioclimatic-habitat species distribution models and maritime-inland connectivity. NeoBiota 109: 177–201. https://doi.org/10.3897/neobiota.109.192296

Introduction

Non-native insects that become invasive in their introduced range are amongst the leading drivers of forest and urban-tree decline worldwide (Brockerhoff and Liebhold 2017). Wood-boring beetles (Coleoptera) are particularly damaging because some species can attack living trees, disrupt timber and fruit production and generate large management costs due to severe ecological and economic impacts when established outside their native range (Lovett et al. 2016; Kenis et al. 2017; Linnakoski and Forbes 2019; Haubrock et al. 2021). The increase in container shipping and movement of wood-packaging material since 1980 have resulted in a corresponding increase in detection of wood-boring insects in recent decades (Aukema et al. 2010). Cryptic invaders that include several longhorn beetles (Cerambycidae), jewel beetles (Buprestidae) and bark and ambrosia beetles (Curculionidae, Scolytinae), have repeatedly been transported outside their native ranges through global trade, often in wood or wood-packaging material (Haack 2006; Lantschner et al. 2020; Ruzzier et al. 2023a). Such repeated introductions facilitate successful establishments (Brockerhoff et al. 2014), underscoring the central role of international trade in facilitating biological invasions and the importance of stringent phytosanitary measures, early detection and rapid response strategies to mitigate ecological and economic impacts (Brockerhoff and Liebhold 2017; Epanchin-Niell et al. 2021; Wray et al. 2024). Preventing the arrival of non-native insects and their early detection are significantly more cost-effective than post-establishment control, making risk-based tools that predict where an organism could survive and reproduce outside its native range essential to plant health planning (Epanchin-Niell et al. 2014; Blaalid et al. 2021).

Species distribution models (SDMs) are used to identify the relationship between species and environmental conditions (Guisan et al. 2017). They can serve as useful tools to produce habitat- and climate-suitability maps for invasive taxa, including Cerambycidae (e.g. Shatz et al. (2016); Krishnankutty et al. (2020); Zhao et al. (2023a, 2023b); Kim et al. (2025)). SDMs can, therefore, provide information for surveillance prioritisation, pathway risk assessments and scenario testing under climate change. When combined with information on trade pathways, host availability and dispersal, they support targeted inspections, quarantine zoning and contingency planning (e.g. Soubeyrand et al. (2024)). However, SDMs must be applied with caution when modelling invasive species. Sampling bias and georeferencing accuracy in occurrence data, the allocation of pseudo-absence/background points, covariate selection, the omission of biotic interactions and dispersal limitations and uncertainty in climate scenarios can all hinder model transferability, leading to an over- or underestimation of areas potentially susceptible to invasion (e.g. Yates et al. (2018); Rousseau and Betts (2022); Valavi et al. (2022); Adde et al. (2023)).

The spatial heterogeneity of climate, host availability and the distribution of trade hubs across Europe creates a complex mosaic of sites with variable invasion risks for non-native cerambycid beetles (e.g. Roques et al. (2020); Rosace et al. (2025)). As a consequence, multiple non-native cerambycids potentially threaten European forestry, urban trees and fruit production (e.g. Malumphy et al. (2020); Lupi et al. (2023); Horrocks et al. (2024); Sarto i Monteys et al. (2024)). Moreover, Europe continues to experience repeated incursions of longhorn beetles, representing a significant risk for further establishment and invasion (e.g. Cocquem-

pot and Lindelöw (2010); Keszthelyi et al. (2019); Ruzzier et al. (2020); Seidel et al. (2021); Ruzzier et al. (2023b)). These realities make integrative risk assessment, relying on SDMs, pathway analysis and surveillance data, critical to international and national plant-health strategies.

Recent detections in Europe of two North American cerambycid beetles, the round-headed apple-tree borer, *Saperda candida* Fabricius, 1787 and the elm borer, *Saperda tridentata* Olivier, 1795 (Lamiinae, Saperdini), have placed these species under European surveillance due to their potential threat to plant health on the continent (EFSA PLH Panel et al. 2020; EPPO 2021). *Saperda candida* is native to much of eastern North America, ranging from south-eastern Canada west to central Alberta and south through many U.S. States (Bousquet et al. 2013; Monné and Nearns 2023). Its primary hosts are fruit and ornamental trees in the family Rosaceae, including *Malus*, *Pyrus*, *Crataegus* and *Amelanchier* (Solomon 1995). It has also been reported from *Betula* sp. (Betulaceae) once (Vlasak and Vlasakova 2002), but reports of *Cotoneaster* (Hess, 1940), *Prunus* (Becker, 1918) and *Pyracantha* (Linsley & Chemsak, 1995) as larval hosts have not been substantiated (Maier 2020). Infestations cause extensive tunnelling in trunks and roots, leading to branch dieback and even tree mortality in orchards and nurseries (EPPO 2021). In Europe, *S. candida* has already been detected in the wild, with the first confirmed record in Germany in 2008 (DEFRA 2025; Julius Kühn-Institut 2025). Since then, active eradication measures have been implemented to prevent further establishment and spread (Julius Kühn-Institut 2025). The detection of the species in natural environments highlights its ability to survive outside its native range and indicates a potential risk to fruit crops, ornamental trees and natural vegetation (EPPO 2021).

Saperda tridentata occurs across eastern North America, with records from the United States and southern Canada (Bousquet et al. 2013; Monné and Nearns 2023). It is primarily associated with elm species (e.g. *Ulmus americana*, *U. rubra*, *U. crassifolia*) (Solomon 1995). Early isolated records reporting *Acer* (Harrington 1883) and *Populus* (Washburn 1910) as larval host plants are considered doubtful and their potential role as substrates for larval feeding and development is currently under investigation (Santoiemma et al., personal communication). Damage results from larval feeding beneath the bark, causing bark splitting, frass exudation, canopy thinning and progressive branch decline (EFSA PLH Panel et al. 2020). In contrast to *S. candida*, *S. tridentata* does not have known adventive populations in Europe, despite repeated interceptions in imported *Ulmus* logs from North America (Binazzi et al. 2019). These interceptions underscore the ongoing risk of accidental introduction and establishment through international trade in wood and plant material. The repeated detection of *S. tridentata* in imported materials demonstrates the species' potential for entry and emphasises the need for continued surveillance and early warning systems to prevent establishment and mitigate future impacts. Both species pose a potential invasion risk to Europe through trade in infested wood or live plants, prompting their inclusion in European surveillance and pest risk analyses (EFSA 2020; EPPO 2021). Given their biology with cryptic larval stages inside trunks/roots, multiple suitable hosts, the likelihood of detection is low until damage becomes noticeable.

The present study aimed to assess the invasion risk of *S. candida* and *S. tridentata* in Europe. We hypothesised that Europe provides climatic and habitat conditions similar to those of the native ranges of both species, potentially allowing their establishment. However, invasion risk was expected to increase with the

intensity of commercial trade and transport, for which maritime and inland connectivity provide suitable proxies. We tested these hypotheses by: (1) developing, for both species, a data-driven joint bioclimatic–habitat species distribution model (JBH-SDM), based on two complementary SDMs: a bioclimatic suitability model (BSM) and a habitat suitability model (HSM), both developed using an ensemble framework that explicitly accounted for sampling bias and the georeferencing accuracy of occurrence records; and (2) integrating JBH-SDM predictions with maritime and inland connectivity linking the species' native ranges to potentially invadable (i.e. environmentally suitable) areas in Europe.

Material and methods

Occurrence data and variable selection

Species occurrences

Occurrences of *S. candida* and *S. tridentata* were downloaded from the Global Biodiversity Information Facility and iNaturalist via the *spocc* R package (Owens et al. 2024). Occurrence data from GBIF and iNaturalist used in the SDMs were updated as of 14 December 2025. The datasets were checked for all potential issues (e.g. duplicate records, misidentifications etc.).

For SDMs calibrated in the native range of the species, we used the available occurrence records (686 for *S. candida* and 922 for *S. tridentata*), with geographic coordinates expressed in degrees and a spatial resolution of at least two decimal places. The rationale of the procedure relies on the capability of associating each occurrence with habitat data derived from land cover cartography with a grid resolution of 0.04167° (corresponding to approximately 5 km at the Equator). Before modelling, the occurrences recurring in the calibration area were thinned through the function "thin" of the package *GeoThinneR* (Mestre-Tomás 2025), with a thinning parameter of 5 km in R, version 4.4.2 to remove occurrences within the same raster cell.

Bioclimatic and habitat covariates (elevation, land cover and host plants layer)

Nineteen bioclimatic layers and a digital elevation model (DEM) with a 0.00833° grid resolution (averaged per anni 1970–2000) were obtained from WorldClim 2.1 (http://www.worldclim.com/version2).

Twelve land-cover layers were sourced from the Global 1-km Consensus Land Cover dataset (http://www.earthenv.org), representing the percentage cover of each land-cover class per 30-arc-second (~ 0.00833°) pixel: evergreen/deciduous needleleaf trees (EDNT), evergreen broadleaf trees (EBT), deciduous broadleaf trees (DBT), mixed/other trees (MOT), shrubs (SHR), herbaceous vegetation (HERB), cultivated/managed vegetation (CMV), regularly flooded vegetation (RFV), urban/built-up (BU), barren lands (BR), open waters (OW) and snow/ice (SI). To reduce computational demand, all bioclimatic, elevation and land-cover layers were upscaled to 0.04167° using the "aggregate" function in the *terra* package (Hijmans 2025). For the habitat suitability modelling (HSM), OW was excluded *a priori*.

To evaluate whether host availability could improve habitat suitability model (HSM), we added a host-plants (HP) layer following the approach of Ruzzier et al.

(2024, 2025a, 2025b). For both *Saperda* species, we created a species-specific host-plant layer considering the genus of each of all reported host plants (*Amelanchier* Medik., *Aronia* Medik., *Betula* L., *Hedlundia* Sennikov & Kurtto, *Cotoneaster* Medik., *Crataegus* L., *Cydonia* Mill., *Malus* Mill., *Prunus* L., *Pyrus* L. and *Sorbus* L. for *S. candida*; *Acer* L., *Populus* L. and *Ulmus* L. for *S. tridentata*). Secondary hosts, even when uncertain, were retained to avoid underestimating the host range for each *Saperda* species in both native and potentially invadable areas; this strategy was adopted to account for the possible presence of congeneric (vicariant) plant species in case *Saperda* species were to shift to alternative, phylogenetically related hosts. For each host-plant genus, occurrence records were retrieved from GBIF (accessed 15 September 2025) using the "occ_data" function of the *rgbif* R package (Chamberlain et al. 2025). Records were converted to georeferenced point patterns ("as.ppp") and transformed into density maps via kernel interpolation ("density.ppp"), with kernel bandwidth estimated by "bw.ppl"; all functions were implemented in the *spatstat* R package (Baddeley and Turner 2005; Baddeley et al. 2005). Kernel density maps were log-transformed to reduce the effect of potential oversampling (Ruzzier et al. 2025a, 2025b). All host-plant kernel density maps were then combined into a single layer by retaining, for each grid cell, the maximum density value amongst all host-plant layers. As different host plants may locally replace one another, the maximum value was retained instead of summing all density layers to avoid overestimating local host-plant density. The resulting maximum-density layer was then multiplied by a land-cover layer comprising all land-cover classes associated with the habitats of the host taxa and, where applicable, with cultivated or managed environments (EDNT, EBT, DBT, MOT, SHR, HERB, CMV), thereby reducing overestimation of host-plant distribution. This procedure generated the final host-plant (HP) layer (Suppl. material 3: figs S1, S2).

Before SDMs calibration, all layers were masked (using the "mask" function of the *terra* package) to exclude areas within the native range of both species that are inaccessible due to geographic barriers (e.g. the sea), thereby preventing the allocation of background points or pseudo-absences in those regions. In addition, these layers were cropped to an extent encompassing the native distribution of both *S. candida* and *S. tridentata* (15°N – 60°N, -125°E – -50°E). This extent spans longitudinally and latitudinally to include all continuous areas (i.e. not interrupted by ecological barriers) from the East Coast to the continental divide of the Rocky Mountains and from the southern regions of North America to the subarctic areas of the continent.

Bioclimatic variables exhibiting noisy or bimodal frequencies of observed presence (FOP) were excluded, retaining only predictors that produced ecologically interpretable response curves (Vollering et al. 2019). This screening was conducted using the R package *MIAmaxent* (Vollering et al. 2019). The variables retained after FOP were Bio13 (precipitation of the wettest month), Bio15 (precipitation seasonality), Bio18 (precipitation of the warmest quarter) and Bio19 (precipitation of the coldest quarter) for both species, with the addition of Bio10 (mean temperature of the warmest quarter) for *S. tridentata*.

To reduce collinearity, the bioclimatic variables retained after FOP and the habitat covariates were evaluated separately using variance inflation factor (VIF) analysis with the "vifcor" function of the *usdm* R package (Naimi et al. 2014). In each group, highly correlated variables (Pearson's $|r| > 0.7$) were excluded (Dormann et al. 2013).

Joint bioclimatic–habitat species distribution modelling

The modelling procedure for each species consisted of two distinct modelling pipelines. Each pipeline included two models, a bioclimatic suitability model (BSM) and a habitat suitability model (HSM), which were used to assess the influence of broad-scale predictors (bioclimatic variables) and fine-scale predictors (e.g. land cover, host plants and elevation) on species distributions, respectively. The suitability maps produced by the BSM and HSM were subsequently integrated to generate an overall environmental suitability map.

Pseudo-absence and background points selection

In each modelling pipeline, pseudo-absences (PAs) were generated for BSM, whereas background points (BPs) were used as absence-like data in HSM. Pseudo-absences were used for BSM to effectively sample the broad bioclimatic gradient across the entire modelling domain, thereby improving characterisation of the species' climatic niche. Conversely, BPs were used for HSM to represent local habitat availability around occurrence records, allowing habitat suitability to be estimated within the accessible area, while minimising the influence of broad-scale climatic conditions. In both cases, the total number of PAs or BPs was set to 3 times the number of occurrences (Warton and Shepherd 2010; Renner et al. 2015). For BSM, PAs were generated across a geographical extent encompassing the species' native ranges, as defined above. This choice aimed to evaluate the effects of bioclimatic variables within a continuous landmass, characterised by the absence of ecological barriers (Ruzzier et al. 2025a, 2025b; Ruzzier and Uliana 2025). Within this extent, PAs were allocated with a spatial density inversely proportional to the occurrence points density. To estimate occurrence density, we used the same kernel estimation strategy adopted for host plants. The natural logarithm of the resulting kernel density surface was used to reduce the influence of potential occurrence aggregation/oversampling that could generate local density peaks. The resulting kernel map was then used as a proxy for species abundance in the native calibration area. In contrast, for HSM, BPs were randomly generated within a buffer around occurrence points, with inner and outer radii of 30 km and 300 km, respectively. The inner buffer prevented the placement of BPs too close to occurrence records, thereby reducing the likelihood of allocating BPs within potentially suitable habitats, whereas the outer buffer allowed the exploration of a wide range of environmental conditions without placing BPs beyond the bioclimatic envelope. This procedure was implemented using the "disk" strategy available in the *biomod2* R package (version 4.2-5-2; Thuiller et al. (2024)).

Ensemble modelling and overall suitability map

For both BSM and HSM, five modelling algorithms were implemented using the "bigboss" settings in *biomod2* (version 4.2.5.2), without further manual tuning: Artificial Neural Networks (ANN), Generalised Additive Models (GAM), Generalised Boosting Models (GBM), Random Forest (RF) and Maximum Entropy (MAXNET). Model outputs generated by each algorithm were subsequently combined using an ensemble modelling approach (Araújo and New 2007; Guisan et al. 2017), as implemented in *biomod2*.

BSM used five sets of PAs, whereas HSM employed 10 sets of BPs. All models were validated using a random five-fold cross-validation (80% training and 20% testing), according to the area under (AUC) the receiver operating characteristic curve (ROC) and the true skill statistic (TSS). Model calibration was performed without fixing the random seed. In total, for each species, 125 models were developed for the BSM (5 algorithms × 5 PA sets × 5 CV folds) and 250 models for the HSM (5 algorithms × 10 BP sets × 5 CV folds), all evaluated using both ROC and TSS. Models with a ROC score ≥ 0.8 and a TSS score ≥ 0.6 were retained to build the final ensemble models using the EMwmean method, whereby ensemble predictions were calculated as the weighted mean of individual model predictions with weights assigned proportionally to their respective evaluation scores (ROC or TSS), using a proportional weighting decay.

Variable importance was assessed through a three-run permutation procedure.

Both BSM and HSM were projected on to the calibration area to obtain native habitat and native bioclimatic suitability maps, respectively. BSM and HSM outputs are suitability maps expressed as probabilities of occurrence derived from two independent models. This approach assumes that ecological filters operating at scenopoetic (climatic) and local (habitat) scales contribute independently to species suitability. To obtain an overall suitability map (representing the overall probability of two independent, BSM and HSM, probabilities) that accounts for the simultaneous effects of habitat and bioclimate on species occurrence probability, the BSM and HSM maps were combined as a spatial product (see Ruzzier et al. (2024)).

The predictive performance of these overall suitability maps within the calibration area was then evaluated using the Boyce index (Boyce et al. 2002) implemented within the *modEvA* R package (Barbosa et al. 2013).

The projection of BSM and HSM on to the European (non-native) range (34°N–72°N, -12°E–43°E) and the overall suitability map were realised following the same procedure described above for the native range projection.

To identify potential extrapolation areas in the European projections of the BSM and HSM, we calculated the multivariate environmental similarity surface (MESS) index (Elith et al. 2010) using the *dismo* R package (Hijmans et al. 2024).

Development of the invasion risk map, based on maritime connectivity by vessel traffic and inland infrastructural network

Maritime connectivity between North America and Europe was quantified using the Liner Shipping Bilateral Connectivity Index (LSBCI), available from the United Nations Conference on Trade and Development (UNCTAD; https://unctadstat.unctad.org/datacentre/dataviewer/US.LSBCI). The LSBCI describes the degree of liner shipping connectivity between pairs of countries, based on the structure of the global maritime transport network. In this study, the LSBCI was used as a proxy for the potential propagule pressure associated with maritime trade, under the assumption that stronger shipping connectivity increases the likelihood of species introduction.

Bilateral connectivity values between the United States and European countries and between Canada and European countries, were considered separately. To obtain a more stable estimate of long-term maritime connectivity, while minimising the influence of annual fluctuations, the average LSBCI over the period 2015–2025 was calculated for each country pair.

European ports connected to the United States and Canada were subsequently identified and georeferenced. For each port, maritime connections with the two source countries were classified as either direct or indirect. Ports with direct connections were assigned the corresponding averaged LSBCI value for the respective country pair, whereas ports connected only indirectly received half of that value, to reflect the lower expected contribution of indirect shipping routes to propagule transfer (Suppl. material 1).

Finally, a maritime connectivity index was calculated for each European port by summing its weighted connectivity with the United States and Canada. This index was used as a spatial proxy for the potential propagule pressure associated with maritime trade and served as the basis for transferring connectivity values to the European terrestrial transport network.

European road and railway networks were obtained from the Natural Earth database using the *rnaturalearth* package in R (Massicotte and South 2026). The vector layers were clipped to the European extent, geometries were validated and all spatial data were projected to the ETRS89 / Lambert Azimuthal Equal Area coordinate system (EPSG:3035) to ensure accurate distance calculations. The road and railway layers were subsequently merged into a single transport network representing the major terrestrial transport infrastructure across Europe.

The centroid of each road and railway segment was used as a representative location and Euclidean distances between all transport segments and European ports were calculated using the *sf* package in R (Pebesma 2018). The contribution of each port to every transport segment was weighted using a negative exponential distance-decay function (l = 200 km; to account for propagule pressure within an infrastructure network in which goods are transported over relatively long distances), assuming that the influence of maritime propagule pressure decreases with increasing distance from the port. The weighted contributions from all ports were subsequently summed to obtain a cumulative connectivity value for each transport segment.

The transport network was then intersected with the European landmass to remove offshore sections and rasterised to a 5-km spatial resolution using the *terra* package, ensuring consistency with the resolution of the species' overall suitability maps. Raster cells intersecting the transport network retained the cumulative connectivity value assigned to the corresponding transport segment.

To generate a continuous map of propagule pressure given by inland connectivity, the Euclidean distance from every terrestrial raster cell to the nearest transport segment was calculated. Each raster cell inherited the connectivity value of its nearest transport segment, which was subsequently reduced according to a second negative exponential distance-decay function to account for the decreasing influence of transport infrastructure with increasing distance (l = 100 km; to prevent overlapping effects from different segments in areas with a high infrastructure density). This procedure assumes that propagules introduced through maritime trade are subsequently dispersed along the terrestrial transport network and that the probability of dispersal decreases progressively away from major transport corridors.

The resulting propagule pressure map was multiplied with the European overall suitability maps for *S. candida* and *S. tridentata* to obtain the two maps of invasion risk.

Results

SDM performance, effect of covariates and transferability

For both *S. candida* and *S. tridentata*, BSMs and HSMs exhibited strong predictive performance, based on cross-validation metrics (Suppl. material 2: tables S1–S4). For *S. candida*, all BSM models (125 of 125; 100%) achieved both ROC scores ≥ 0.8 and TSS values ≥ 0.6. Similarly, for the HSMs, although some models did not meet the predefined validation thresholds, the overall modelling performance remained very high: ROC scores resulted ≥ 0.8 in 248 of 250 cases (99.2%), while 227 of 250 models (90.8%) reached a TSS ≥ 0.6. For *S. tridentata*, BSM, ROC scores ≥ 0.8 were obtained in all models (125 of 125; 100%) and 122 of 125 models (97.6%) achieved a TSS ≥ 0.6. For the HSM, models achieved ROC scores ≥ 0.8 in all cases (250 of 250; 100%), whereas only 106 of 250 models (42.4%) reached a TSS ≥ 0.6.

The ensemble modelling procedure provided variable importance scores and response curves for both species (Suppl. material 2: tables S5–S8; Suppl. material 3: figs S5–S8).

Bioclimatic suitability for both species was primarily associated with precipitation seasonality (coefficient of variation), which showed the highest relative importance (0.72 for *S. candida* and 0.61 for *S. tridentata*; Suppl. material 3: figs S5, S6). Additional variables with high relative importance included precipitation of the warmest quarter (0.41) for *S. candida* and mean temperature of the warmest quarter (0.55) together with precipitation of the warmest quarter (0.24) for *S. tridentata*. Overall, higher predicted suitability for both species was associated with humid temperate climatic conditions, characterised by relatively high and evenly distributed precipitation throughout the year. For *S. tridentata*, mean temperature of the warmest quarter also showed high relative importance. Model response curves indicated that higher predicted suitability was associated with mean temperatures of the warmest quarter exceeding approximately 18 °C, with predicted suitability increasing as temperature increased.

For *S. candida*, predicted occurrence probability was most strongly associated with host plants (importance = 0.64), followed by cultivated/managed vegetation (0.32), evergreen/deciduous needleleaf trees (0.27) and herbaceous vegetation (0.26) (Suppl. material 3: fig. S7). Response curves indicated a positive association between host plants and predicted occurrence probability, whereas cultivated/managed vegetation, evergreen/deciduous needleleaf trees and herbaceous vegetation were negatively associated with predicted occurrence probability.

For *S. tridentata*, predicted occurrence probability was most strongly associated with host plants (importance = 0.53), followed by mixed/other trees (0.42), cultivated/managed vegetation (0.24), the digital elevation model (0.24), herbaceous vegetation (0.15) and evergreen/deciduous needleleaf trees (0.12) (Suppl. material 3: fig. S8). Response curves indicated a positive association between host plants and predicted occurrence probability, whereas all remaining variables were negatively associated with predicted occurrence probability.

Within their respective calibration areas, ROC and TSS projection maps for both BSM and HSM exhibited very high internal consistency (Pearson's correlation coefficients always > 0.99 for both species); therefore, we presented only the

ROC maps. Bioclimatic and habitat suitability maps, together with their 95% confidence intervals, are presented in Suppl. material 3: figs S11–S14.

The overall suitability maps of each species showed excellent calibration according to the Boyce index. Boyce index values reached 0.998 for both *S. candida* and *S. tridentata*, indicating strong agreement between observed occurrences and predicted suitability (Suppl. material 3: figs S9, S10).

MESS analyses revealed that extrapolations for BSM and HSM were negligible across the European projections for both species (Suppl. material 3: figs S15, S16).

These results indicate that the JBH-SDM framework provides robust and transferable predictions across both native ranges that could be credible for the potential invadable European ranges.

JBH-SDM – projections

Saperda candida: species suitability for the native range

Bioclimatic suitability. The bioclimatic suitability map identified a broad and largely continuous area of moderate to high suitability across eastern North America (Suppl. material 3: fig. S11), extending from the south-eastern to the north-eastern United States and parts of the Midwest. Suitability progressively declined towards western and more continental regions.

Habitat suitability. Habitat suitability showed a heterogeneous and fragmented spatial pattern (Suppl. material 3: fig. S13). High suitability was concentrated in the eastern United States, particularly along the Appalachian Region, the eastern Midwest and the north-eastern forested areas, whereas large portions of North America exhibited low or negligible suitability.

Overall suitability. Compared with the bioclimatic suitability projection, the overall suitability map showed a reduced extent of highly suitable areas, with habitat acting as a limiting factor and producing a more spatially structured pattern of suitability (Fig. 1A). The highest suitability values remained concentrated in the eastern United States and showed strong spatial correspondence with known occurrence records (Boyce index; Suppl. material 3: fig. S9).

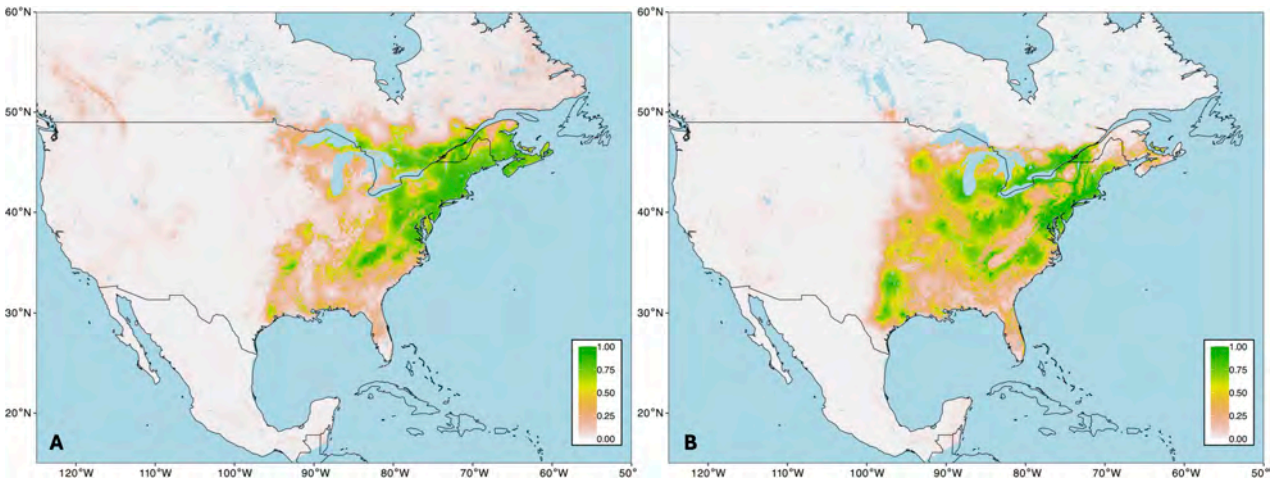

Figure 1. Overall suitability map (native range) of *Saperda candida* (**A**) and *S. tridentata* (**B**). Colours represent predicted suitability, ranging from low (white) to high (green).

Saperda tridentata: species suitability for the native range

Bioclimatic suitability. The bioclimatic suitability map identified a broad and largely continuous area of high suitability across eastern North America (Suppl. material 3: fig. S12), extending throughout most of the eastern United States, including the south-eastern region, the Midwest and the north-eastern areas. Suitability gradually declined towards western and more continental regions.

Habitat suitability. Habitat suitability showed a heterogeneous, but relatively continuous spatial pattern across the eastern portion of North America (Suppl. material 3: fig. S14). High suitability was predicted throughout much of the eastern United States, extending from the south-eastern region through the Midwest to the north-eastern forested areas, with an additional narrow belt of suitable habitat along the western coast of North America. Spatial discontinuities were evident within parts of the eastern United States, although extensive suitable areas remained connected.

Overall suitability. Compared with the bioclimatic suitability projection, the overall suitability map showed a reduced extent of suitable areas, with habitat acting as a limiting factor and producing a more spatially structured pattern of suitability (Fig. 1B). Moderate to high suitability remained concentrated across the eastern United States, extending from the south-eastern region through the Midwest to the north-eastern areas and showed strong spatial correspondence with observed occurrence records (Boyce index; Suppl. material 3: fig. S10).

Saperda candida: species suitability for Europe

Bioclimatic suitability. The bioclimatic suitability map identified a spatially restricted pattern of suitability across Europe (Suppl. material 3: fig. S17). High suitability was concentrated in western and central Europe, particularly across eastern France, southern Germany, Switzerland, Austria, northern Italy and parts of the western Balkans. Additional areas of moderate suitability occurred in the British Isles and parts of the Atlantic and Alpine regions, whereas northern, eastern and southern Europe were generally characterised by low suitability.

Habitat suitability. Habitat suitability map showed a rather broad and continuous spatial pattern (Suppl. material 3: fig. S18). High suitability extended across much of western and central Europe, including France, Belgium, the Netherlands, Luxembourg, Germany, Switzerland, Austria, northern Italy, the British Isles, northern Spain and parts of southern Scandinavia.

Overall suitability. The overall suitability map identifies spatially structured potentially invadable areas for *S. candida* across Europe (Fig. 2A). The most suitable areas are concentrated in a core region spanning eastern France, Belgium, the Netherlands, Luxembourg, southern and western Germany, Switzerland, Austria and northern Italy, forming a continuous belt of highly suitable areas across central Europe; outside this core area, suitability declines progressively. Moderate suitability extends into parts of western France, the British Isles, southern Scandinavia and the western Balkans, reflecting either locally favourable habitat conditions or climatically suitable pockets. In contrast, in Eastern Europe and northern Fennoscandia, the joint influence of bioclimate and habitat conditions determines the availability of suitable areas, whereas in southern Europe, bioclimate acts as the primary limiting factor governing the extent of the overall suitability.

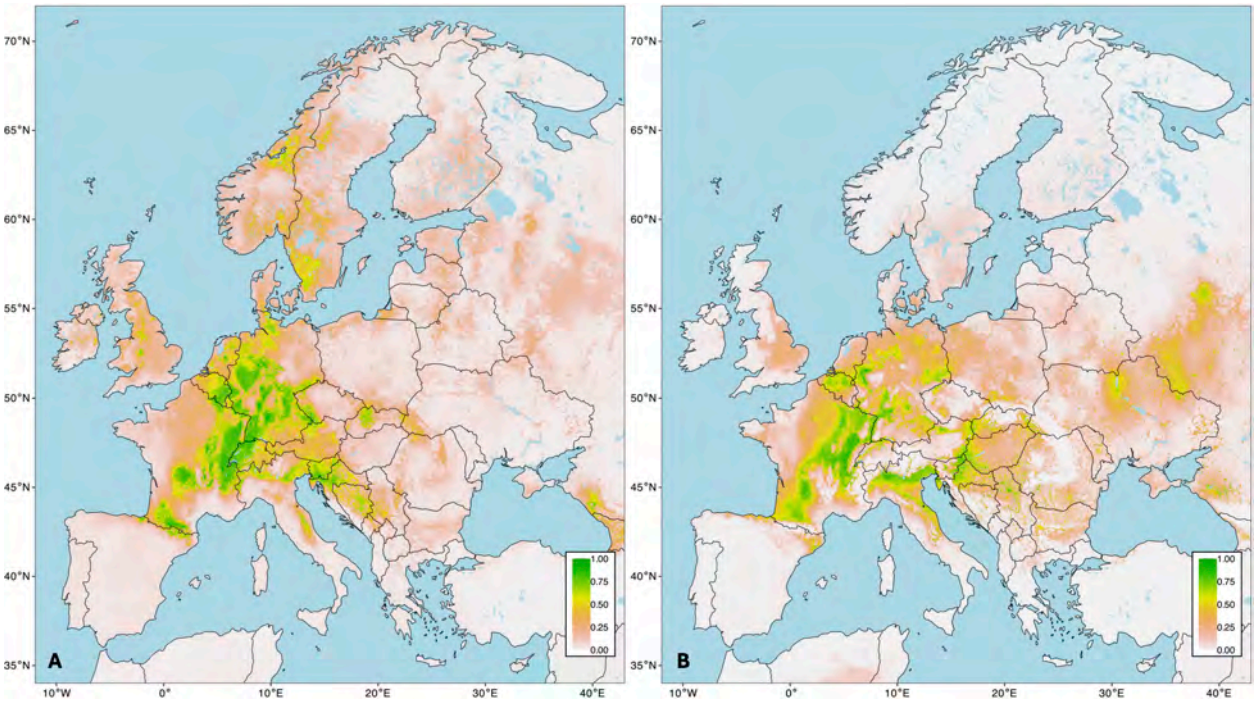

Figure 2. Predicted overall suitability of *S. candida* (**A**) and *S. tridentata* (**B**). Colours represent predicted suitability, ranging from low (white) to high (green).

Saperda tridentata: species suitability for Europe

Bioclimatic suitability. The bioclimatic suitability map identified broad and largely continuous areas of high suitability across much of Europe (Suppl. material 3: fig. S19). High suitability extended from western through central and eastern Europe, whereas lower suitability occurred in northern Europe, mountainous regions and the southernmost Mediterranean areas.

Habitat suitability. The habitat suitability map showed a spatially structured, but relatively continuous pattern across Europe (Suppl. material 3: fig. S20). High suitability was predicted across large portions of western and central Europe, including France, Germany, northern Italy and parts of eastern Europe, while localised reductions were mainly associated with mountainous regions.

Overall suitability. Areas of moderate to high overall suitability were concentrated across western and central Europe (Fig. 2B). Compared to the habitat projection alone, the extent of suitable areas was reduced, although remaining broadly continuous across the continent. Several regions, characterised by high habitat suitability, exhibited lower overall suitability, reflecting the effect of bioclimate as a limiting factor. Nevertheless, large and connected regions of moderate to high overall suitability persisted across Europe, indicating extensive areas where habitat and climate are jointly predicted to be suitable for *S. tridentata*.

Risk assessment

The propagule pressure map shows a high level of interconnection and consequently high propagule pressure, between the native ranges of both *Saperda* species and the European countries bordering the Atlantic Ocean, except for the Scandinavian Peninsula and Ireland. High propagule pressure is also observed for Italy and the north-eastern part of the Adriatic coast (Fig. 3).

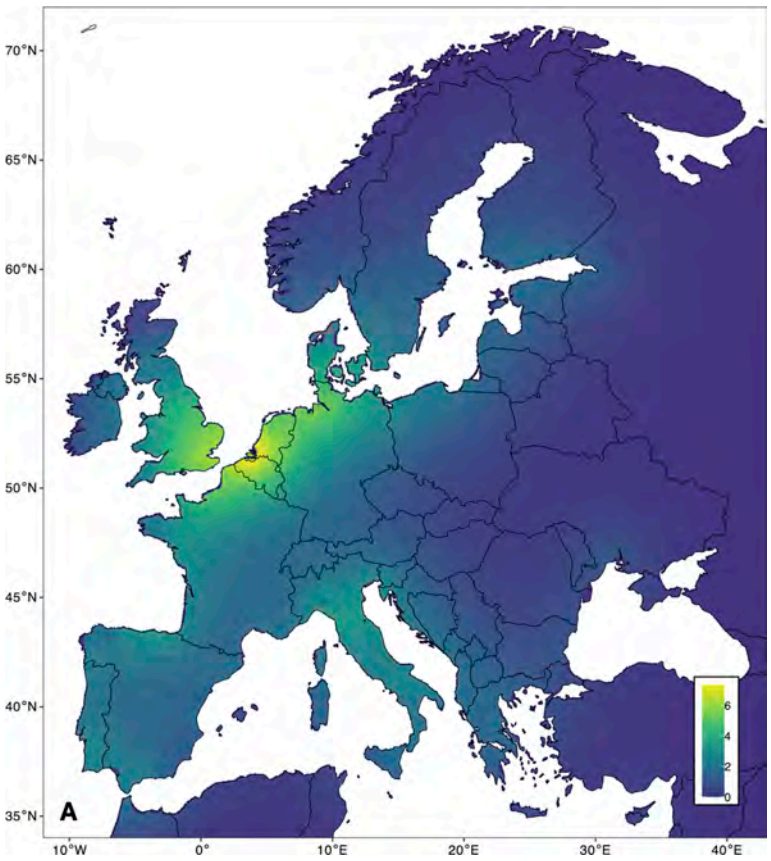

Figure 3. Spatial representation of propagule pressure across Europe obtained by combining maritime connectivity (Liner Shipping Bilateral Connectivity Index, LSBCI) with inland transport network connectivity (roads and railways). Warmer colours indicate higher estimated propagule pressure, whereas cooler colours indicate lower estimated propagule pressure.

The integration of environmental suitability with maritime connectivity between the USA/Canada and Europe, together with European inland transport connectivity (road and railway networks), provides a spatially explicit assessment of the invasion risk posed by *S. candida* and *S. tridentata* across Europe. Although environmentally suitable conditions occur over extensive areas, the resulting invasion risk maps reveal strong spatial heterogeneity, with the highest invasion risk occurring where high environmental suitability coincides with major maritime connections and densely interconnected road and railway networks.

For *S. candida*, the highest invasion risk forms an extensive and largely continuous core across western and central Europe (Fig. 4A). High invasion risk extends from northern and eastern France through Belgium, the Netherlands and Luxembourg into much of Germany, Switzerland and northern Italy. Elevated risk is also evident in south-western France and north-eastern Spain, particularly along the Pyrenean Region. Outside this main core, distinct high-risk areas occur across much of England and Wales, along the northern and eastern Adriatic coast, particularly in north-eastern Italy, Slovenia and Croatia and in southern Sweden. These geographically separated hotspots indicate that high invasion risk is not restricted to the central European corridor, but also occurs in regions combining suitable conditions with major coastal gateways and well-developed inland transport connections.

For *S. tridentata*, the highest-risk area is similarly centred on western and central Europe, but displays a somewhat different spatial configuration (Fig. 4B). A broad,

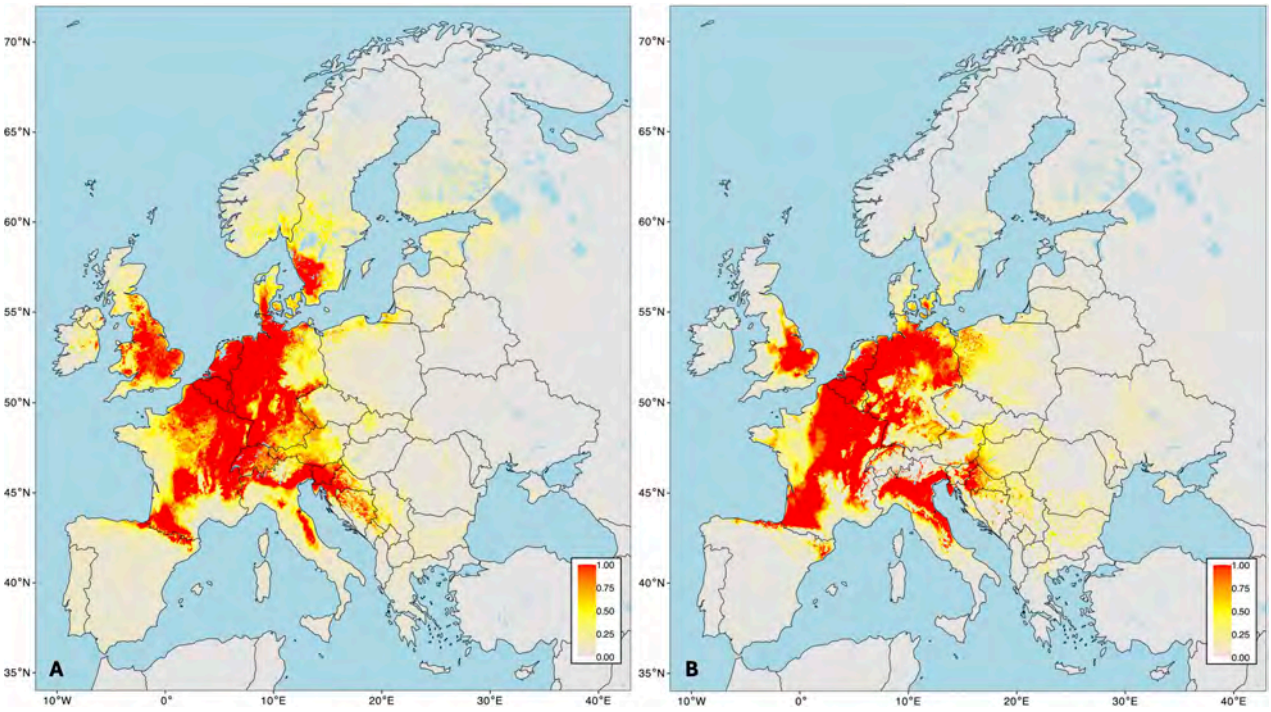

Figure 4. Invasion risk maps of *S. candida* (**A**) and *S. tridentata* (**B**). Warmer colours denote higher invasion risk, whereas cooler colours denote lower invasion risk.

highly connected zone extends from north-eastern France through Belgium, the Netherlands and Luxembourg, across Germany and Switzerland and into northern and central Italy. High values also occur along the Atlantic coast of southern western France. In Great Britain, the principal hotspot is more geographically restricted than for *S. candida* and is concentrated mainly in central eastern England. Elevated risk is also present around the northern Adriatic and along parts of the Croatian coast, although it is more fragmented and less extended than that predicted for *S. candida*. In contrast, the pronounced hotspot observed in southern Sweden for *S. candida* is almost absent for *S. tridentata*.

Overall, the two species share a major high-risk core across western and central Europe, but differ in the extent and spatial continuity of secondary hotspots. These differences suggest that species-specific environmental responses modulate the spatial consequences of exposure to a shared transport network. In this context, maritime connectivity facilitates long-distance introductions, whereas road and railway networks promote subsequent inland dispersal.

Discussion

The modelling framework we employed in this study showed strong overall performance, delivering consistent and robust predictions for both *Saperda* species across their native ranges as well as for projections in Europe. Forecasting invasion risk is key to effectively managing invasive species (Thomas et al. 2024), although limitations and challenges of SDMs have been questioned (Barbet-Massin et al. 2018; Lee-Yaw et al. 2022; Fenollosa et al. 2025). Our modelling framework allowed us to evaluate separately the effect of scenopoetic variables and local variables on the ecological niche of the investigated species, thereby avoiding potential confounding effects in reconstructing the two niche components (bioclimatic and habitat-related)

that may arise when jointly considering variables describing processes operating at different spatial scales, as previously highlighted by Adde et al. (2023) and Ruzzier et al. (2024, 2025a, 2025b). This modelling approach is particularly important when estimating the actual climatic and habitat suitability in areas that are potentially invadable and differ from those used for model calibration (i.e. the native range).

Moreover, a particularly important aspect concerns modelling, based exclusively on presence data within the species' native range; such occurrences can be assumed to reflect a species distribution of a population that is in equilibrium with the environment as a whole (Hui 2023). Consequently, this allows for the estimation of the realized niche occupied by the species within its native range and the identification of areas outside this range where analogous environmental conditions occur. In addition, for species whose biology is closely associated with a specific set of host plants, including these variables in habitat modelling further improved the ability to identify and refine suitability at a local scale.

While the joint bioclimatic–habitat models identified extensive areas of environmental suitability across Europe, the invasion-risk maps revealed a more spatially structured pattern. Rather than being uniformly distributed across all environmentally suitable regions, the highest invasion risk became concentrated within a limited number of geographically coherent hotspots where suitable environmental conditions overlapped with high values of transport-based proxies of propagule pressure. This framework highlights the added value of integrating environmental suitability with these proxies, allowing environmentally suitable areas to be distinguished from those that also exhibit greater potential for introduction and subsequent spread.

The modelled native range of *S. candida* primarily encompasses eastern North America, extending from the south-eastern and central-eastern United States to the Midwest and north-eastern regions, with partial inclusion of adjacent areas in southern Canada. Bioclimatic models indicate a strong association with humid temperate climates, characterised by low precipitation seasonality and relatively stable conditions throughout the year. In particular, *S. candida* is closely associated with stable precipitation regimes and high moisture availability during the warmest quarter. These results are consistent with suitability assessments reported by EPPO (2021). From a habitat perspective, the species is strongly linked to the availability of host plants, which represents the primary constraint on its distribution. It is narrowly associated with host-dominated forest habitats, avoiding cultivated and managed areas lacking host plants, as well as coniferous forests. Overall, its native range corresponds predominantly to mesic temperate forests of eastern North America, where suitable climatic conditions and host availability co-occur. When projected to Europe, *S. candida* shows a wide extent of suitable and relatively continuous areas, largely driven by the distribution of host plants and associated land-cover types. However, bioclimatic projections alone indicate a more restricted suitability, suggesting that climate may act as a filtering factor. In particular, the species appears more strongly associated with the moister climates of central Europe, characterised by precipitation distributed throughout the year.

The modelled native range of *S. tridentata* largely overlaps with that of *S. candida*, encompassing eastern North America from the south-eastern and central-eastern United States to the Midwest and north-eastern regions, with some extension into southern Canada. Similarly, bioclimatic models indicate an association with humid temperate climates and low precipitation seasonality. However, *S. tridentata* shows a greater association with temperature conditions, occurring across temper-

ate to warm environments during the warmest quarter, suggesting a stronger influence of temperature gradients in shaping its climatic niche. These findings are also consistent with EFSA PLH Panel et al. (2020). As for habitat, the species remains dependent on host plant availability, but exhibits a broader ecological tolerance compared to *S. candida*, occurring in mixed forests and, to a limited extent, in cultivated and managed areas, with a preference for low-elevation environments. As with *S. candida*, its native distribution reflects the overlap between suitable climate and host availability within mesic temperate forests. When projected to Europe, *S. tridentata* also shows extensive areas of potential suitability driven by host plant distribution. However, bioclimatic projections indicate a more constrained pattern, highlighting the role of climate as a limiting factor. In Europe, the species appears associated with milder and more temperate conditions, such as those found in central Italy. Nevertheless, the potential host plant range still requires further investigation, as precise information on host use is currently lacking. Indeed, *Ulmus* is currently the only confirmed host genus, whereas the inclusion of *Acer* and *Populus* is based on sporadic occurrence records rather than confirmed host associations (Washburn 1910; EFSA 2020).

Overall, for both species, habitat availability emerges as a primary environmental filter within the native range, while climate plays a stronger constraining role in shaping potential areas of establishment under a European invasion scenario. This pattern is consistent with findings for other invasive longhorn beetles, such as *Aromia bungii* (Faldermann, 1835) (Cerambycinae, Callichromatini) and *Psacothea hilaris* (Pascoe, 1857) (Lamiinae, Monochamini), for which host plant availability represents a key determinant of distribution (Ruzzier et al. 2024, 2025a). Moreover, habitat may be even more limiting; indeed, habitat suitability may be slightly overestimated due to the inclusion in the HSM of host plants whose use by the two *Saperda* species remains to be verified.

Considering the results presented in this study, the current presence of *S. candida* on the island of Fehmarn (northern Germany) represents a clear phytosanitary concern. This situation is consistent with previous assessments by competent authorities and fully supports the inclusion of the species in the European Union A1 Quarantine Pest list (Annex II A). Our modelling results provide quantitative and spatially explicit evidence that reinforces the high-risk status attributed to this species.

The invasion-risk map identifies a broad high-risk corridor extending across western and central Europe, including much of Germany and neighbouring countries. Several of these high-risk areas occur in close proximity to the current outbreak on Fehmarn, potentially increasing the likelihood of further spread if containment and eradication measures prove unsuccessful. The continuity of environmentally suitable habitats, together with the high connectivity characterising these regions, suggests that *S. candida* could establish and persist over extensive areas of continental Europe if propagules disperse from the current infestation site, either naturally or through human-mediated movement of infested materials. Propagule pressure is, in fact, a key factor influencing the establishment and spread of non-native species (Brockerhoff et al. 2014).

However, the comparatively moderate suitability predicted for the island of Fehmarn suggests that containment and eradication measures could be successfully implemented. The predominance of agricultural land use reduces habitat continuity and the availability of host plants required to sustain populations capable of generating high propagule pressure. Moreover, the local bioclimatic conditions,

although not entirely unfavourable, are less suitable than those predicted for the neighbouring continental high-risk areas. Together, these factors indicate that the currently established population likely occurs under ecologically marginal conditions, where both long-term persistence and spatial expansion are constrained. Under such circumstances, the timely implementation of targeted phytosanitary measures could substantially increase the likelihood of complete eradication.

The elevated invasion risk predicted for *S. tridentata* across western and central Europe, together with the sustained and well-documented propagule pressure resulting from repeated interceptions (Binazzi et al. 2019), indicates that continued vigilance is necessary to prevent its establishment in Europe. In particular, the predicted high-risk corridor extending from France through Belgium, the Netherlands and Luxembourg to Germany, Switzerland and northern Italy, together with secondary hotspots in eastern England and along the northern Adriatic coast, identifies priority areas where surveillance and early detection efforts should be concentrated. For both species, the comparison between overall suitability and invasion-risk maps demonstrates that environmental suitability alone does not fully explain the geography of invasion risk. Although environmentally suitable conditions occur across extensive portions of Europe, invasion risk is highest in hotspots where favourable environmental conditions coincide with intense transport connectivity. Both species share a broad high-risk core across western and central Europe, but differ in the extent and distribution of secondary hotspots. In particular, *S. candida* exhibits more extensive high-risk areas across Great Britain, southern Sweden and the northern Adriatic Region, whereas *S. tridentata* remains more strongly concentrated within the central European corridor. These differences indicate that species-specific environmental responses continue to shape the spatial pattern of invasion risk despite both species sharing similar introduction pathways.

We acknowledge that the outputs outlined here represent a potential invasion scenario that does not account for possible limiting factors within European ecosystems that could counteract the invasion process. Amongst these, biotic resistance may play a key role. For instance, the presence of native congeners in invaded areas may limit the establishment and spread of non-native species, as natural enemies associated with native congeners could shift hosts and regulate populations of introduced relatives, preventing rapid spread or high population densities (Cavender-Bares et al. 2009; Dearborn et al. 2016). In Europe, nine species and three subspecies of the genus *Saperda* are currently recorded. If *S. candida* and *S. tridentata* were to become sympatric with native *Saperda* spp., interactions with the resident community could potentially reduce their invasiveness. Similar dynamics have been observed following the establishment of the European brown spruce longhorned beetle, *Tetropium fuscum* (Fabricius, 1787), in eastern Canada, where native natural enemies contributed to limiting its population growth (Dearborn et al. 2016; Heustis et al. 2018).

Conclusions

The risk maps produced in this study indicate a substantial potential for both *Saperda* species to establish and spread across Europe, although invasion risk is far from uniform. The highest-risk areas are concentrated within a broad western and central European corridor, where favourable environmental conditions, widespread host availability and intense maritime and terrestrial connectivity con-

verge. Additional regional hotspots, particularly in Great Britain, the northern Adriatic Region and, for *S. candida*, southern Sweden, further demonstrate that invasion risk extends beyond the main continental core. Conversely, large portions of northern, eastern and southern Europe remain characterised by comparatively low invasion risk, reflecting lower environmental suitability, weaker transport connectivity or a combination of both.

Taken together, these results demonstrate that, although Europe offers extensive environmentally suitable areas for both *S. candida* and *S. tridentata*, environmental suitability alone does not fully explain the geography of invasion risk. The integration of transport connectivity concentrates the highest-risk areas into a limited number of geographically coherent hotspots, providing a more realistic representation of where introduction and establishment are most likely to occur. This finding underscores the limitations of suitability-based projections alone and highlights the added value of integrated risk frameworks that explicitly incorporate dispersal pathways. Such approaches provide a more robust and operational basis for prioritising surveillance, early detection and preventative phytosanitary measures, ultimately supporting more effective management of invasive wood-boring insects.

Acknowledgements

The authors express their sincere gratitude to the reviewers and the editor for their thorough and expert evaluation, which has substantially enhanced the quality and clarity of the manuscript.

References

Adde A, Rey PL, Brun P, Külling N, Fopp F, Altermatt F, Broennimann O, Lehmann A, Petitpierre B, Zimmermann NE, Pellissier L, Guisan A (2023) N-SDM: A high-performance computing pipeline for nested species distribution modelling. Ecography 2023: e06540. https://doi.org/10.1111/ecog.06540

Araújo MB, New M (2007) Ensemble forecasting of species distributions. Trends in Ecology and Evolution 22(1): 42–47. https://doi.org/10.1016/j.tree.2006.09.010

Aukema JE, McCullough DG, Von Holle B, Liebhold AM, Britton K, Frankel SJ (2010) Historical accumulation of nonindigenous forest pests in the continental United States. BioScience 60(11): 886–897. https://doi.org/10.1525/bio.2010.60.11.5

Baddeley A, Turner R (2005) spatstat: An R package for analysing spatial point patterns. Journal of Statistical Software 12(6). https://doi.org/10.18637/jss.v012.i06

Baddeley A, Rubak E, Turner R (2005) Spatial Point Patterns: Methodology and Applications with R. CRC Press, Boca Raton, 826 pp.

Barbet-Massin M, Rome Q, Villemant C, Courchamp F (2018) Can species distribution models really predict the expansion of invasive species? PLOS ONE 13(3): e0193085. https://doi.org/10.1371/journal.pone.0193085

Barbosa AM, Real R, Muñoz AR, Brown JA (2013) New measures for assessing model equilibrium and prediction mismatch in species distribution models. Diversity and Distributions 19(11): 1333–1338. https://doi.org/10.1111/ddi.12100

Becker GG (1918) The round-headed apple-tree borer. *Saperda candida* Fab. University of Arkansas, Agricultural Experiment Station Bulletin 146: 1–93.

Binazzi F, Del Nista D, Sabbatini Peverieri G, Marianelli L, Roversi PF, Pennacchio F (2019) *Saperda tridentata* Olivier (Coleoptera Cerambycidae Lamiinae): Continuous interceptions at the Italian

port of Livorno represent a growing challenge for phytosanitary services. Redia 102: 171–176. https://doi.org/10.19263/REDIA-102.19.24

Blaalid R, Magnussen K, Westberg N B, Navrud S (2021) A benefit-cost analysis framework for prioritization of control programs for well-established invasive alien species. NeoBiota 68: 31–52. https://doi.org/10.3897/neobiota.68.62122

Bousquet Y, Bouchard P, Davies AE, Sikes DS (2013) Checklist of beetles (Coleoptera) of Canada and Alaska (2nd edn.). Pensoft Series Faunistica 109: 1–402. https://doi.org/10.3897/zookeys.360.4742

Boyce MS, Vernier PR, Nielsen SE, Schmiegelow FKA (2002) Evaluating resource selection functions. Ecological Modelling 157(2–3): 281–300. https://doi.org/10.1016/S0304-3800(02)00200-4

Brockerhoff EG, Liebhold AM (2017) Ecology of forest insect invasions. Biological Invasions 19(11): 3141–3159. https://doi.org/10.1007/s10530-017-1514-1

Brockerhoff EG, Kimberley M, Liebhold AM, Haack RA, Cavey JF (2014) Predicting how altering propagule pressure changes establishment rates of biological invaders across species pools. Ecology 95(3): 594–601. https://doi.org/10.1890/13-0465.1

Cavender-Bares J, Kozak KH, Fine PVA, Kembel SW (2009) The merging of community ecology and phylogenetic biology. Ecology Letters 12: 693–715. https://doi.org/10.1111/j.1461-0248.2009.01314.x

Chamberlain S, Barve V, Mcglinn D, Oldoni D, Desmet P, Geffert L, Ram K (2025) rgbif: Interface to the Global Biodiversity Information Facility API. R package version 3.8.1. https://doi.org/10.32614/cran.package.rgbif

Cocquempot C, Lindelöw Å (2010) Longhorn beetles (Coleoptera, Cerambycidae). BioRisk 4: 193–218. https://doi.org/10.3897/biorisk.4.56

Dearborn KW, Heard SB, Sweeney J, Pureswaran DS (2016) Displacement of *Tetropium cinnamopterum* (Coleoptera: Cerambycidae) by its invasive congener *Tetropium fuscum*. Environmental Entomology 45(4): 848–854. https://doi.org/10.1093/ee/nvw045

DEFRA (2025) Round-headed apple tree borer (*Saperda candida*) [factsheet]. https://planthealthportal.defra.gov.uk/assets/factsheets/Saperda-candida-July-2025-v3-final.pdf [Accessed 17 March 2026]

Dormann CF, Elith J, Bacher S, Buchmann C, Carl G, Carré G, García Marquéz JR, Gruber B, Lafourcade B, Leitão PJ, Münkemüller T, McClean C, Osborne PE, Reineking B, Schröder B, Skidmore AK, Zurell D, Lautenbach S (2013) Collinearity: A review of methods to deal with it and a simulation study evaluating their performance. Ecography 36(1): 27–46. https://doi.org/10.1111/j.1600-0587.2012.07348.x

EFSA PLH Panel [EFSA Panel on Plant Health], Bragard C, Dehnen-Schmutz K, Di Serio F, Gonthier P, Jacques M-A, Jaques Miret JA, Justesen AF, MacLeod A, Magnusson CS, Milonas P, Navas-Cortes JA, Parnell S, Potting R, Reignault PL, Van der Werf W, Civera AV, Yuen J, Zappala L, Evans H, Maiorano A, Thulke H-H (2020) Scientific opinion on the pest categorisation of *Saperda tridentata*. EFSA Journal 18(1): e5940. https://doi.org/10.2903/j.efsa.2020.5940

Elith J, Kearney M, Phillips S (2010) The art of modelling range-shifting species. Methods in Ecology and Evolution 1(4): 330–342. https://doi.org/10.1111/j.2041-210X.2010.00036.x

Epanchin-Niell R, McAusland C, Liebhold A, Mwebaze P, Springborn MR (2021) Biological invasions and international trade: Managing a moving target. Review of Environmental Economics and Policy 15(1): 180–190. https://doi.org/10.1086/713025

Epanchin-Niell RS, Brockerhoff EG, Kean JM, Turner JA (2014) Designing cost-efficient surveillance for early detection and control of multiple biological invaders. Ecological Applications 24(5): 1258–1278. https://doi.org/10.1890/13-1331.1

EPPO (2021) Report of a pest risk analysis for *Saperda candida*. European and Mediterranean Plant Protection Organization, Paris, France. https://pra.eppo.int/pra/864693f9-3476-4573-b47d-2cf4750bcead

Fenollosa E, Pang SEH, Briscoe NJ, Guisan A, Salguero-Gómez R (2025) Powerful yet challenging: Mechanistic niche models for predicting invasive species potential distribution under climate change. Ecography: e07775. https://doi.org/10.1002/ecog.07775

Guisan A, Thuiller W, Zimmermann NE (2017) Habitat suitability and distribution models: With applications in R. Cambridge University Press, Cambridge, 514 pp. https://doi.org/10.1017/9781139028271

Haack RA (2006) Exotic bark- and wood-boring Coleoptera in the United States: Recent establishments and interceptions. Canadian Journal of Forest Research 36(2): 269–288. https://doi.org/10.1139/x05-249

Harrington WH (1883) Correspondence. The Canadian Entomologist 15: 79–80. https://doi.org/10.4039/Ent1579-4

Haubrock PJ, Turbelin AJ, Cuthbert RN, Novoa A, Taylor NG, Angulo E, Ballesteros-Mejia L, Bodey TW, Capinha C, Diagne C, Essl F, Golivets M, Kirichenko N, Kourantidou M, Leroy B, Renault D, Verbrugge L, Courchamp F (2021) Economic costs of invasive alien species across Europe. NeoBiota 67: 153–190. https://doi.org/10.3897/neobiota.67.58196

Hess AD (1940) The biology and control of the roundheaded apple-tree borer, *Saperda candida* Fabricius. New York (Geneva) Agricultural Experiment Station Bulletin 688: 1–93.

Heustis A, Moise ER, Johns R, Pureswaran DS, Heard SB (2018) Impact of an invasive longhorned beetle, *Tetropium fuscum* (Coleoptera: Cerambycidae), on community structure of subcortical and wood-associated insects in Eastern Canada. Environmental Entomology 47(1): 39–47. https://doi.org/10.1093/ee/nvx190

Hijmans R (2025) terra: Spatial data analysis. R package version 1.8-29. https://doi.org/10.32614/cran.package.terra

Hijmans R, Phillips S, Leathwick J, Elith J (2024) dismo: Species distribution modeling. R package version 1.3-16. https://doi.org/10.1016/b978-0-12-822562-2.00379-0

Horrocks KJ, Zhang J, Haye T, Seehausen ML, Maggini R, Xian X, Xu Z, Wang H, Zou Y, Li Z, Wan F, Gariepy TD (2024) Biology, impact, management and potential distribution of *Aromia bungii*, a major threat to fruit crops around the world. Journal of Pest Science 97: 1725–1747. https://doi.org/10.1007/s10340-024-01767-0

Hui C (2023) The dos and don'ts for predicting invasion dynamics with species distribution models. Biological Invasions 25(4): 947–953. https://doi.org/10.1007/s10530-022-02976-3

Julius Kühn-Institut (2025) Update of an outbreak of *Saperda candida* in Germany (Schleswig-Holstein) [pest report]. https://pflanzengesundheit.julius-kuehn.de/dokumente/upload/Saperda_candida_pr2025-02-17_SH.pdf [Accessed 17 March 2026]

Kenis M, Roques A, Santini A, Liebhold AM (2017) Impact of non-native invertebrates and pathogens on market forest tree resources. In: Vilà M, Hulme PE (Eds) Impact of Biological Invasions on Ecosystem Services. Springer, 103–117. https://doi.org/10.1007/978-3-319-45121-3_7

Keszthelyi S, Fehér B, Somfalvi-Tóth K (2019) Worldwide distribution and theoretical spreading of *Trichoferus campestris* (Coleoptera: Cerambycidae) depending on the main climatic elements. Entomological Science 22: 339–352. https://doi.org/10.1111/ens.12375

Kim MJ, Lee SK, Park Y, Kim YH, Lee MG, Nam Y (2025) Climatic suitability and spread potential of *Anoplophora horsfieldii* (Coleoptera: Cerambycidae), a newly identified non-native insect on Jeju Island, Korea. Scientific Reports 15: e10428. https://doi.org/10.1038/s41598-025-95652-0

Krishnankutty SM, Bigsby K, Hastings J, Takeuchi Y, Wu Y, Lingafelter SW, Ray AM (2020) Predicting establishment potential of an invasive wood-boring beetle, *Trichoferus campestris* (Coleoptera: Cerambycidae), in the United States. Annals of the Entomological Society of America 113: 88–99. https://doi.org/10.1093/aesa/saz051

Lantschner MV, Corley JC, Liebhold AM (2020) Drivers of global Scolytinae invasion patterns. Ecological Applications 30: e02103. https://doi.org/10.1002/eap.2103

Lee-Yaw JA, McCune JL, Pironon S, Sheth SN (2022) Species distribution models rarely predict the biology of real populations. Ecography 2022: e05877. https://doi.org/10.1111/ecog.05877

Linnakoski R, Forbes KM (2019) Pathogens–The hidden face of forest invasions by wood-boring insect pests. Frontiers in Plant Science 10: e90. https://doi.org/10.3389/fpls.2019.00090

Linsley EG, Chemsak JA (1995) The Cerambycidae of North America, part VII, no. 2: Taxonomy and classification of the subfamily Lamiinae, tribes Acanthocinini through Hemilophini. University of California Publications in Entomology 114: 1–292.

Lovett GM, Weiss M, Liebhold AM, Holmes T, Leung B, Lambert KF, Orwig DA, Campbell FT, Rosenthal J, McCullough DG, Wildova R, Ayres MP, Canham CD, Foster DR, LaDeau SL, Weldy T (2016) Nonnative forest insects and pathogens in the United States: Impacts and policy options. Ecological Applications 26: 1437–1455. https://doi.org/10.1890/15-1176

Lupi D, Malabusini S, De Milato S, Heinzl AL, Ruzzier E, Bani L, Faccoli M, Casale S, Jucker C (2023) Exploring the range expansion of the yellow-spotted longhorn beetle *Psacothea hilaris hilaris* in northern Italy. Agricultural and Forest Entomology 25: 511–521. https://doi.org/10.1111/afe.12570

Maier CT (2020) Larval hosts of Lamiine Cerambycidae (Coleoptera) in Connecticut and nearby states. The Coleopterists Bulletin 74: 77–92. https://doi.org/10.1649/0010-065X-74.1.77

Malumphy C, Guillem R, Perez C, Bensusan K (2020) Insect pest species of *Eucalyptus* in Gibraltar. Entomologist's Monthly Magazine 156: 51–57. https://doi.org/10.31184/m00138908.1561.4010

Massicotte P, South A (2026) rnaturalearth: World map data from Natural Earth. R package version 1.2.0. https://doi.org/10.32614/CRAN.package.rnaturalearth

Mestre-Tomás J (2025) GeoThinneR: Efficient spatial thinning of species occurrences. R package version 2.0.0. https://doi.org/10.32614/CRAN.package.GeoThinneR

Monné MA, Nearns EH (2023) Catalogue of the Cerambycidae (Coleoptera) of Canada and United States of America. Part IV. Subfamily Lamiinae [online]. http://cerambycids.com/catalog/Monne&Nearns_Jan2024_NearcticCat_part_IV.pdf [Accessed 10 December 2025]

Naimi B, Hamm NA, Groen TA, Skidmore AK, Toxopeus AG (2014) Where is positional uncertainty a problem for species distribution modelling? Ecography 37: 191–203. https://doi.org/10.1111/j.1600-0587.2013.00205.x

Owens H, Barve V, Chamberlain S (2024) spocc: Interface to species occurrence data sources. R package version 1.2.3. https://doi.org/10.32614/CRAN.package.spocc

Pebesma E (2018) Simple features for R: Standardized support for spatial vector data. The R Journal 10: 439–446. https://doi.org/10.32614/RJ-2018-009

Renner IW, Elith J, Baddeley A, Fithian W, Hastie T, Phillips SJ, Popovic G, Warton DI (2015) Point process models for presence-only analysis. Methods in Ecology and Evolution 6: 366–379. https://doi.org/10.1111/2041-210X.12352

Roques A, Auger-Rozenberg MA, Ren L (2020) Are invasive patterns of non-native insects related to woody plants differing between Europe and China? Frontiers in Forests and Global Change 2: e91. https://doi.org/10.3389/ffgc.2019.00091

Rosace MC, Bohan DA, Dufour MC (2025) Hotspot mapping of pest introductions in the EU: A regional analysis of environmental, anthropogenic, and spatial effects. Biological Invasions 27: 781–795. https://doi.org/10.1007/s10530-024-03461-9

Rousseau JS, Betts MG (2022) Factors influencing transferability in species distribution models. Ecography 2022: e06060. https://doi.org/10.1111/ecog.06060

Ruzzier E, Uliana M (2025) *Cassida piperata* (Coleoptera, Chrysomelidae), a non-native beetle, new to Italy and Europe. Biodiversity Data Journal 13: e177770. https://doi.org/10.3897/BDJ.13.e177770

Ruzzier E, Morin L, Glerean P, Forbicioni L (2020) New and interesting records of Coleoptera from northeastern Italy and Slovenia. The Coleopterists Bulletin 74: 523–531. https://doi.org/10.1649/0010-065X-74.3.523

Ruzzier E, Haack RA, Curletti G, Roques A, Volkovitsh MG, Battisti A (2023a) Jewels on the go: Exotic buprestids around the world (Coleoptera, Buprestidae). Neobiota 84: 107–135. https://doi.org/10.3897/neobiota.84.90829

Ruzzier E, De Queros CR, Mas H, Di Giulio A (2023b) Simultaneous detections of *Olenecamptus bilobus* in Europe. Biodiversity Data Journal 11: e114432. https://doi.org/10.3897/BDJ.11.e114432

Ruzzier E, Lupi D, Tirozzi P, Dondina O, Orioli V, Jucker C, Bani L (2024) A two-step species distribution modeling to disentangle the effect of habitat and bioclimatic covariates on *Psacothea hilaris*. Biological Invasions 26: 1861–1881. https://doi.org/10.1007/s10530-024-03283-9

Ruzzier E, Lee S, Tirozzi P, Orioli V, Di Giulio A, Dondina O, Bani L (2025a) The role of host plants, land cover and bioclimate in predicting the invasiveness of *Aromia bungii* on a global scale. Scientific Reports 15: e2353. https://doi.org/10.1038/s41598-025-86616-5

Ruzzier E, Scaccini D, Tirozzi P, Orioli V, Dondina O, Di Giulio A, Pozzebon A, Bani L (2025b) Predicting the global distribution and invasion scenarios of *Lycorma delicatula*. NeoBiota 103: 267–298. https://doi.org/10.3897/neobiota.103.154246

Sarto i Monteys V, Savin I, Tutusaus GT, Balsach MB (2024) New evidence on the spread in Catalonia of *Xylotrechus chinensis* and the efficacy of abamectin control. Scientific Reports 14: e26754. https://doi.org/10.1038/s41598-024-78265-x

Seidel M, Lüttke M, Cocquempot C, Potts K, Heeney W, Husemann M (2021) Citizen scientists significantly improve our knowledge on *Chlorophorus annularis* in Europe. BioRisk 16: 1–13. https://doi.org/10.3897/biorisk.16.61099

Shatz AJ, Rogan J, Sangermano F, Miller J, Elmes A (2016) Modeling the risk of spread and establishment for Asian longhorned beetle (*Anoplophora glabripennis*) in Massachusetts. Geocarto International 31: 813–831. https://doi.org/10.1080/10106049.2015.1086901

Solomon JD (1995) Guide to Insect Borers in North American Broadleaf Trees and Shrubs. USDA Forest Service, Washington DC, 735 pp.

Soubeyrand S, Estoup A, Cruaud A, Malembic-Maher S, Meynard C, Ravigné V, Barbier M, Barrès B, Berthier K, Boitard S, Dallot S, Gaba S, Grosdidier M, Hannachi M, Jacques MA, Leclerc M, Lucas P, Martinetti D, Mougel C, Robert C, Roques A, Rossi JP, Suffert F, Abad P, Auger-Rozenberg MA, Ay JS, Bardin M, Bernard H, Bohan DA, Candresse T, Castagnone-Serreno P, Danchin EGJ, Delmas CEL, Ezanno P, Fabre F, Facon B, Gabriel E, Gaudin J, Gauffre B, Gautier M, Guinat C, Lavigne C, Lemaire O, Martinez C, Michel L, Moury B, Nam K, Nédellec C, Ogliastro M, Papaïx J, Parisey N, Poggi S, Radici A, Rasplus JY, Reboud X, Robin C, Roche M, Rusch A, Sauvion N, Streito JC, Verdin E, Walker AS, Xuéreb A, Thébaud G, Morris CE (2024) Building integrated plant health surveillance: A proactive research agenda. CABI Agriculture and Bioscience 5: 1–72. https://doi.org/10.1186/s43170-024-00273-8

Thomas SM, Verhoeven MR, Walsh JR, Larkin DJ, Hansen GJ (2024) Improving species distribution forecasts by measuring and communicating uncertainty. Ecology 105: e4297. https://doi.org/10.1002/ecy.4297

Thuiller W, Georges D, Gueguen M, Engler R, Breiner F, Lafourcade B, Patin R, Blancheteau H (2024) biomod2: Ensemble Platform for Species Distribution Modeling. R package version 4.2-5-2. https://biomodhub.github.io/biomod2/ https://doi.org/10.32614/cran.package.biomod2

Valavi R, Guillera-Arroita G, Lahoz-Monfort JJ, Elith J (2022) Predictive performance of presence-only species distribution models. Ecological Monographs 92: e01486. https://doi.org/10.1002/ecm.1486

Vlasak J, Vlasakova K (2002) Records of Cerambycidae (Coleoptera) in Massachusetts with notes on larval hosts. The Coleopterists Bulletin 56: 203–219. https://doi.org/10.1649/0010-065X(2002)056[0203:ROCCIM]2.0.CO;2

Vollering J, Halvorsen R, Mazzoni S (2019) The MIAmaxent R package: Variable transformation and model selection for species distribution models. Ecology and Evolution 9: 12051–12068. https://doi.org/10.1002/ece3.5654

Warton DI, Shepherd LC (2010) Poisson point process models solve the "pseudo-absence problem" for presence-only data. The Annals of Applied Statistics 4: 1383–1402. https://doi.org/10.1214/10-AOAS331

Washburn FL (1910) Thirteenth Report of the State Entomologist of Minnesota (1909–1910). University of Minnesota Agricultural Experiment Station, 152 pp.

Wray AK, Agnew AC, Brown ME, Dean EM, Hernandez ND, Jordon A, Morningstar C, Piccolomini SE, Pickett HA, Daniel W, Reichert BE (2024) Understanding gaps in early detection of and rapid response to invasive species. Ecological Informatics 84: e102855. https://doi.org/10.1016/j.ecoinf.2024.102855

Yates KL, Bouchet PJ, Caley MJ, Mengersen K, Randin CF, Parnell S, Fielding AH, Bamford AJ, Ban S, Barbosa AM, Dormann CF, Elith J, Embling CB, Ervin GN, Fisher R, Gould S, Graf RF, Gregr EJ, Halpin PN, Heikkinen RK, Heinänen S, Jones AR, Krishnakumar PK, Lauria V, Lozano-Montes H, Mannocci L, Mellin C, Mesgaran MB, Moreno-Amat E, Mormede S, Novaczek E, Oppel S, Ortuño Crespo G, Peterson AT, Rapacciuolo G, Roberts JJ, Ross RE, Scales KL, Schoeman D, Snelgrove P, Sundblad G, Thuiller W, Torres LG, Verbruggen H, Wang L, Wenger S, Whittingham MJ, Zharikov Y, Zurell D, Sequeira AM (2018) Outstanding challenges in the transferability of ecological models. Trends in Ecology and Evolution 33: 790–802. https://doi.org/10.1016/j.tree.2018.08.001

Zhao H, Xian X, Liang T, Wan F, Shi J, Liu W (2023a) Constructing an ensemble model and niche comparison for *Phoracantha semipunctata*. Insects 14: 1–84. https://doi.org/10.3390/insects14010084

Zhao J, Zou X, Yuan F, Luo Y, Shi J (2023b) Predicting the current and future distribution of *Monochamus carolinensis*. Pest Management Science 79: 5393–5404. https://doi.org/10.1002/ps.7753

Zurell D, Franklin J, König C, Bouchet PJ, Dormann CF, Elith J, Fandos G, Feng X, Guillera-Arroita G, Guisan A, Lahoz-Monfort JJ, Leitão PJ, Park DS, Peterson AT, Rapacciuolo G, Schmatz DR, Schröder B, Serra-Diaz JM, Thuiller W, Yates KL, Zimmermann NE, Merow C (2020) A standard protocol for reporting species distribution models. Ecography 43: 1261–1277. https://doi.org/10.1111/ecog.04960

Additional information

Conflict of interest

The authors have declared that no competing interests exist.

Ethical statement

No ethical statement was reported.

Artificial Intelligence (AI) use

The authors accept full responsibility for the content of the manuscript, including the disclosure of any use of AI.
Regarding the use of AI in the preparation of this manuscript, the authors declare the following: GPT, used for assistance with language, style and writing.

Funding

ER, ADG, LB acknowledge the support of NBFC to University of Roma Tre, Department of Science and to University of Milano-Bicocca, Department of Earth and Environmental Sciences. Funder: Project funded under the National Recovery and Resilience Plan (NRRP), Mission 4 Component 2 Investment 1.4 – Call for tender No. 3138 of 16 December 2021, rectified by Decree n.3175 of 18 December 2021 of the Italian Ministry of University and Research funded by the European Union – NextGenerationEU. Award Number: Project title "National Biodiversity Future Center –NBFC", Project code CN_00000033, Concession Decree No. 1034 of 17 June 2022 adopted by the Italian Ministry of University and Research, CUP: F83C22000730006, CUP: H43C22000530001. DR, JS, GS, DP were supported by the project "Saperda tridentata on European elms and other tree species – SAPTREES", funded by EFSA (European Food Safety Authority) under the call GP/EFSA/ALPHA/2021/07 – Lot 1.

Author contributions

All authors have contributed equally.

Author ORCIDs

E. Ruzzier https://orcid.org/0000-0003-1020-1247
D. Rassati https://orcid.org/0000-0001-7778-0349
A. Di Giulio https://orcid.org/0000-0003-0508-0751
G. Santoiemma https://orcid.org/0000-0002-3226-9253
D.S. Pureswaran https://orcid.org/0000-0002-4040-7708
J. Sweeney https://orcid.org/0000-0003-3391-2375
L. Bani https://orcid.org/0000-0001-5795-9499

Data availability

All data supporting the findings of this study are available in the main text and the Suppl. materials 1–3. The R scripts, relevant spatial layers, GeoTIFF files and ODMAP (Zurell et al. 2020) are freely available on Zenodo (https://doi.org/10.5281/zenodo.21406645).

Supplementary material 1

European ports connected to the United States and Canada

Authors: Enrico Ruzzier, Davide Rassati, Andrea Di Giulio, Giacomo Santoiemma, Deepa S. Pureswaran, Jon Sweeney, Luciano Bani

Data type: xlsx

Link: https://doi.org/10.3897/neobiota.109.192296.suppl1

Supplementary material 2

Excel file including single model performances and variables importance

Authors: Enrico Ruzzier, Davide Rassati, Andrea Di Giulio, Giacomo Santoiemma, Deepa S. Pureswaran, Jon Sweeney, Luciano Bani

Data type: xlsx

Explanation note: **table S1.** *Saperda candida* – Evaluation HSM. Table of the two evaluation metrics used for HSM. **table S2.** *Saperda candida* – Evaluation BSM. Table of the two evaluation metrics used for BSM. **table S3.** *Saperda tridentata* – Evaluation HSM. Table of the two evaluation metrics used for HSM. **table S4.** *Saperda tridentata* – Evaluation BSM. Table of the two evaluation metrics used for BSM. **table S5.** *Saperda candida* - Importance of the covariates included in the HSM. **table S6.** *Saperda candida* -Importance of the covariates included in the BSM. **table S7.** *Saperda tridentata* - Importance of the covariates included in the HSM. **table S8.** *Saperda tridentata* -Importance of the covariates included in the BSM.

Link: https://doi.org/10.3897/neobiota.109.192296.suppl2

Supplementary material 3

Variable response curves, prediction and projection maps, MESS

Authors: Enrico Ruzzier, Davide Rassati, Andrea Di Giulio, Giacomo Santoiemma, Deepa S. Pureswaran, Jon Sweeney, Luciano Bani

Data type: pdf

Explanation note: **fig. S1.** Spatial distribution of the maximum kernel density of host plants (HP.max) of *S. candida* in North America. **fig. S2.** Spatial distribution of the maximum kernel density of host plants (HP.max) of *S. candida* in Europe. **fig. S3.** Spatial distribution of the maximum kernel density of host plants (HP.max) of *S. tridentata* in North America. **fig. S4.** Spatial distribution of the maximum kernel density of host plants (HP.max) of *S. tridentata* in Europe. **fig. S5.** Response curves of covariates included in the *S. candida* bioclimatic suitability model (BSM) obtained from the two evaluation metrics (ROC in green, TSS in red). **fig. S6.** Response curves of covariates included in the *S. tridentata* bioclimatic suitability model (BSM) obtained from the two evaluation metrics (ROC in green, TSS in red). **fig. S7.** Response curves of covariates included in the *S. candida* habitat suitability model (HSM) obtained from the two evaluation metrics (ROC in green, TSS in red). **fig. S8.** Response curves of covariates included in the *S. tridentata* habitat suitability model (HSM) obtained from the two evaluation metrics (ROC in green, TSS in red). **fig. S9.** Boyce index of the overall suitability map of *S. candida* native range. **fig. S10.** Boyce index of the overall suitability map of *S. tridentata* native range. **fig. S11.** Bioclimatic suitability map for *S. candida* in its native range obtained projecting the bioclimatic suitability model (BSM); a) lower limit of the 95% confidence interval; b) mean; c) upper limit of the 95% confidence interval. **fig. S12.** Bioclimatic suitability map for *S. tridentata* in its native range obtained projecting the bioclimatic suitability model (BSM); a) lower limit of the 95% confidence interval; b) mean; c) upper limit of the 95% confidence interval. **fig. S13.** Habitat suitability map for *S. candida* in its native range obtained projecting the habitat suitability model (HSM); a) lower limit of the 95% confidence interval; b) mean; c) upper limit of the 95% confidence interval. **fig. S14.** Habitat suitability map for *S. tridentata* in its native range obtained projecting the habitat suitability model (HSM); a) lower limit of the 95% confidence interval; b) mean; c) upper limit of the 95% confidence interval. **fig. S15.** *Saperda candida*: Multivariate Environmental Similarity Surfaces (MESS) index for Europe. **fig. S16.** *Saperda tridentata*: Multivariate Environmental Similarity Surfaces (MESS) index for Europe. **fig. S17.** Bioclimatic suitability maps for *S. candida* across Europe, generated by projecting the bioclimatic suitability model (BSM): (a) lower 95% confidence limit; (b) mean suitability; (c) upper 95% confidence limit. **fig. S18.** Habitat suitability maps for *S. candida* across Europe, generated by projecting the habitat suitability model (HSM): (a) lower 95% confidence limit; (b) mean suitability; (c) upper 95% confidence limit. **fig. S19.** Bioclimatic suitability maps for *S. tridentata* across Europe, generated by projecting the bioclimatic suitability model (BSM): (a) lower 95% confidence limit; (b) mean suitability; (c) upper 95% confidence limit. **fig. S20.** Habitat suitability maps for *S. tridentata* across Europe, generated by projecting the habitat suitability model (HSM): (a) lower 95% confidence limit; (b) mean suitability; (c) upper 95% confidence limit.

Link: https://doi.org/10.3897/neobiota.109.192296.suppl3